Journal of Hazardous Materials 164 (2009) 1030–1035

Contents lists available at ScienceDirect

Journal of Hazardous Materials

journal homepage: www.elsevier.com/locate/jhazmat

Detection and discrimination of low concentration explosives using MOS nanoparticle sensors

Yanghai Gui [a,*], Changsheng Xie [b], Jiaqiang Xu [a], Guoqing Wang [a]

[a] Henan Provincial Key Laboratory of Surface & Interface Science, Zhengzhou University of Light Industry, Zhengzhou 450002, PR China
[b] The State Key Laboratory of Plastic Forming Simulation and Mould Technology, Department of Materials science and Engineering, Huazhong University of Science and Technology, Wuhan 430074, PR China

ARTICLE INFO

Article history:
Received 20 July 2008
Received in revised form 1 September 2008
Accepted 1 September 2008
Available online 10 September 2008

Keywords:
Explosive
Electronic nose
Doped-ZnO nanoparticle
Sensor arrays
DFA

ABSTRACT

In the present study, four explosives of NH_4NO_3, mineral explosives (ME), picric acid (PA) and 2,6-dinitrotoluene (2,6-DNT) have been investigated by using ZnO-doped nanoparticle sensors with additives of Sb_2O_3, TiO_2, V_2O_5 and WO_3. Firstly, eighteen ZnO-doped nanoparticle sensors were optimized and selected six best sensors to compose a new optimized array. Then, the detection capability of the sensor array was studied by using static sampling method. The results showed that with the increase in concentration of samples, the sensitivities of the sensors also increased, and the lowest detection limit of the four samples were low to 3.34 μg/L. At last, for the sake of approaching closer practical application, these four explosives were also studied with full dynamic sampling method and the results demonstrated that all the samples could be well identified completely at the concentration of 15.4 μg/L when maximum values of slope were extracted as the feature parameters to DFA analysis.

1. Introduction

It is believed that the terrorist attacks of September 11, 2001 have impacts on the daily life in the USA, and also worldwide [1]. In fact, the September 11 attacks is only the fleck of the terrorist activities in the lately past years, such as bombings of buses in Israel and the Phillipines, commuter trains in Spain, and two passenger jets in Russia, etc. [2]. As noted above revealed that law enforcement agencies throughout the world are faced with the problem of detecting hidden bombs in luggage, mail, vehicles, aircraft, as well as on suspects, with the surge of international terrorism and the increased use of explosives in terrorist attacks [3].

At present, canines have been trained and used successfully for sniffing out the hidden explosives; however, dogs are expensive to train and are easily tired [4]. Some analytical instruments including gas chromatography coupled to a mass spectrometer, neutron activation analysis, and electron capture detection are also employed to the specific explosive or its signal vapours [5,6]. Although these techniques are highly selective, they are cumbersome and not easily fielded in a small, low power package, and take much long time to report the analytical results. Metal detectors should be the initial and traditional method to check the bombs but they are becoming increasingly unreliable because the amount of metal used in modern bombs is becoming very small or completed rubber bombs. Therefore, the development of more compact, low-cost and efficient instruments is highly desired for facilitating the task of on-site monitoring of explosives. The developing technique of electronic nose can meet the desire, which mimics the bomb-sniffing dogs without their drawbacks. Many electronic nose techniques for detection of explosives have been reviewed in Refs. [3,7]. An electronic nose (eNose) is usually composed of a chemical sensing system and a pattern-recognition system, such as an artificial neural network. Metal oxide semiconductor (MOS) gas sensor is one class of the electronic noses and usually reported as detectors for VOCs (volatile organic compounds) because of its sensitivity, low-cost and easy manufacturing [8–10]. But to our knowledge, there are a small number of papers reported on the MOS sensors for detection of solid explosives up to now [11,12]. In Ref. [11], Pardo et al. investigated the problem of sensing military grade TNT and some substrates (air, sand and soil) by using tin dioxide thin film sensors with a static headspace sampling, which indicated that using MOS sensors to detect solid explosive was a feasible method. For the detection of solid explosives, however, the low vapour concentration makes it an extremely difficult and challenging problem [13]. To solve this problem, some researchers suggested platinum or palladium catalyst in the carrier gas line to increase the sensitivity of the MOS sensors, and the important thing is that it can allow the

* Corresponding author. Tel.: +86 13298177341; fax: +86 37163556510.
E-mail address: yhgui@zzuli.edu.cn (Y. Gui).

0304-3894/$ – see front matter.
doi:10.1016/j.jhazmat.2008.09.011

Table 1
The components of the raw materials and thick film processing for the optimized sensors.

Number of sensor	Components of raw material	Thick film processing
1	Zn (1% $PdCl_2$)	Prepared from Zn nanoparticle flurry and then quickly immerge the dry film into 1% $PdCl_2$ solution and out. And sintered as described in Section 2.1
2	Zn	Prepared from Zn nanoparticle flurry. And sintered as described in Section 2.1
3	1 at% TiO_2 + Zn	Prepared from mixture flurry of TiO_2 and Zn nanoparticles in atom ratio of Ti to Zn of 1:99. And sintered as described in Section 2.1
4	1 at% WO_3 + Zn	Prepared from mixture flurry of WO_3 and Zn nanoparticles in atom ratio of W to Zn of 1:99. And sintered as described in Section 2.1
5	5 at% V_2O_5 + Zn (1% $PdCl_2$)	Prepared from mixture flurry of V_2O_5 and Zn nanoparticles in atom ratio of V to Zn of 5:95 and then quickly immerged into 1% $PdCl_2$ solution and out. And sintered as described in Section 2.1
6	5 at% Sb_2O_3 + Zn	Prepared from mixture flurry of Sb_2O_3 and Zn nanoparticles in atom ratio of Sb to Zn of 5:95. And sintered as described in Section 2.1

sampling of solids and liquids as well as gases with a gas sensor [4,14].

In the present study, ZnO and the doping ZnO-based nanoparticle sensors were employed to detect the four representative explosives viz 2,6-DNT, NH_4NO_3, picric acid (PA) and solid explosive for mining (ME). Firstly, the dynamic sampling method was employed to optimize the sensor arrays, and then uses the optimized array to test the detection capability of the sensors for the four explosives with static sampling method. At last, for the sake of approaching practical application, low concentration of explosives were investigated with the full dynamic sampling method.

2. Experimental

2.1. Sensors preparation

Zinc nanoparticles used as zinc sources and some oxide dopants such as Sb_2O_3, TiO_2, V_2O_5 and WO_3 were employed to prepare ZnO and ZnO-based doping thick film sensors. The Zn nanoparticles were obtained by thermal evaporation methods, with mean size of 35 nm and purity of 99.99% [15]. All the dopants are of analytical reagent grade. These powders were completely mixed with different atom ratios of 0%, 1%, 5%, 10% dopants and some processed with 1% $PdCl_2$ solution (optimized sensors' information shown in Table 1) and made flurry to be coated on Al_2O_3 tubes on which Pt electrode wires had been fixed at each end. The thick films were sintered at 650 °C for 2 h after drying in air to remove water. Structure phase and image characterizations showed that these film materials had been transformed into pure ZnO and doped-ZnO nanomaterials after sintering. These sensors can be used after aging.

2.2. Experimental methods

2.2.1. Dynamic sampling method to select the better sensors

A steady micro-pump is used to make airflow. 4.0 mg of each explosive is loaded in a ceramic pot in which the Pt–Rh alloy filament with 3.5 V DC power supplier is crimpled. The sensors are placed in the test chamber and operated using a circuit voltage (10 V) at a heater voltage of 5 V. The gas-sensing circuit is similar with that in Ref. [16] and the resistance (R_S) of the sensors could be obtained by using the formula as

$$R_S = \frac{V_c - V_{out}}{V_{out}} R_L \quad (1)$$

where V_c is the circuit voltage; V_{out} the out voltage and R_L the load resistor. The micro-pump is powered on before experiment and went on till to the end. The power of the Pt–Rh alloy filament is turned on after the base-line resistance of all the sensors becomes steady, and the explosive analyte can be catalytically decomposed into CO_x, H_2O and NO_x, etc. Different explosives will produce gas mixture, which has different gas components (fingerprint products). These fingerprint gas molecules are quickly flowed over the sensors in the test chamber where they react with the gas sensors. The structure of the experimental setups in this section is shown in Fig. 1(A). All the eighteen sensors prepared in Section 2.1 were employed to test the fingerprint gas molecules. The signal data can be acquired by personal computer connected with the circuit board in test chamber.

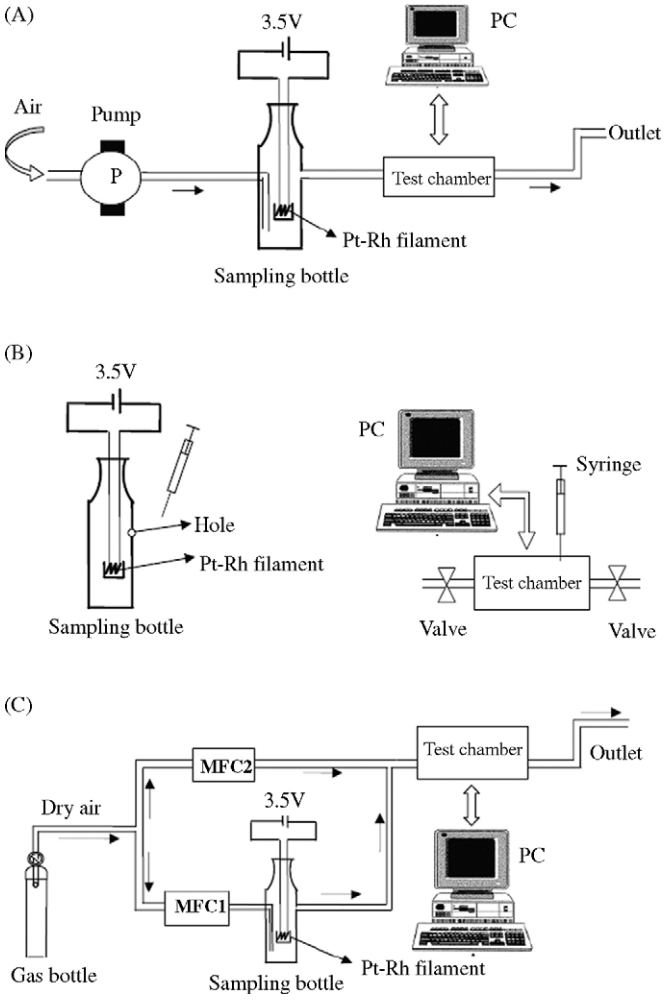

Fig. 1. The structures of the experimental setups: (A) the structure of the dynamic sampling set-up for sensors optimization, (B) the structure of static-state experimental setups, and (C) the structure of the dynamic sampling and low concentration experimental setup.

2.2.2. Static sampling method to test the detection capability of the optimized six sensors for the explosives after Section 2.2.1

This method is similar with the static headspace sampling [11]. The difference is that the catalytically decomposed fingerprint gases of the explosive analyte other than the explosive itself are extracted with a syringe and injected into the test chamber. The test chamber is cleaned with the fresh airflow before and after each test. The sensitivity, S, was defined as R_a/R_g, where R_a and R_g are the electrical resistances of the sensor in air and under exposure to the test gas, respectively. If $R_g > R_a$ then S was defined as R_g/R_a such as 2,6-DNT explosive. The structure of experimental setups of this section is shown in Fig. 1(B).

2.2.3. Dynamic sampling method to simulate practical application for low concentration of explosives

The experimental setup is shown in Fig. 1(C). This equipment is composed of several main parts which are as follows:

- dry air used to cause air flow and to clean the test chamber;
- two mass flow controllers (MFC1, MFC2, Model D07-12AM/ZM) with control units (Model D08-2D/ZM) used to accurately control the gas flows. Through these two gas flows, the concentration of the analytes can be diluted to get different concentration;
- the Pt–Rh alloy filament with 3.5 V DC power supplier crimpled in the ceramic pot in the sampling bottle, the fingerprint gases were caused in this section;
- test chamber with an array of six sensors;
- data acquisition and A/D via the board manufactured by National Instruments and connected with PC.

2.3. Data processing

Appropriate feature parameters extracted from the response curve were used as the input for data analysis algorithms. The convenient classification method of discriminant functional analysis (DFA) was employed for data processing. All data analysis were performed in statistical software SPSS 10.0.

3. Results and discussion

3.1. Sensors optimization

Eighteen sensors prepared by mixing different raw materials were used to test the four analytes. Each measurement was repeated eight times. The typical response curves for the four explosives are plotted in Fig. 2. The 2,6-DNT explosive exhibited reducing signal (Fig. 2(b)), whereas all other three explosives showed oxidizing signals as that of PA (Fig. 2(a)). To select a better sensor array, two feature parameters were considered: one base-line resistance and the other extreme voltage, corresponding to minimum and maximum voltages. The base-line resistance characterizes the stability of the sensor and the extreme voltage characterizes the sensitivity to different analytes. After the eight times tests for all the four explosives, the base-line resistance should be stable and the extreme voltages should reveal huge otherness. The discrete distribution of these 64 values in two groups can be done according to the above two rules. Six best sensors are picked out to form a new optimum array for the desire of further tests. The six sensors are listed in Table 1 marking out their components of raw materials and the thick sensing film processing before sintering.

3.2. Static-state experiments

4.0 mg explosives were weighted out and decomposed in a flask with a volume of 60 ml. An accurate volume of the decomposed products are then extracted with a syringe and injected into the testing chamber with a volume of 4.0 L in which the optimized six sensors are listed (Fig. 1(B)). In the present experiment, the extracted volumes are 0.2, 0.6, 1.0, 3.0, and 5.0 ml corresponding to five different concentrations, respectively. The mass concentration, C_m, of the raw explosives can be obtained as follows:

$$C_m = \frac{(4.0\,\text{mg}/60\,\text{ml})A\,\text{ml}}{4\,\text{L}} \quad (2)$$

where 4.0 mg is the weight of the explosive; 60 ml, the volume of the flask in which the explosive decomposed; 4 L, the volume of testing chamber; A ml, the extracted volume of the decomposed products. Therefore, the values of C_m are 3.34, 10.0, 16.67, 50.0, and 83.34 μg/L corresponding to the extracted volumes of 0.2, 0.6, 1.0, 3.0, and 5.0 ml, respectively. The typical response curves for sensor 3 exposed to the decomposed gas of PA are plotted in Fig. 3. It indicated that the signal increases with the increase of the decomposed gas concentration. Fig. 4 shows the sensitivity of the six sensors to various concentrations of the four explosives. Fig. 4(a)–(d) are for the PA, ME, NH_4NO_3 and 2,6-DNT explosive, respectively. A nonlinear relationship between sensitivity and the concentration was observed on all sensors. Among the four explosives, the gas-sensing signals of NH_4NO_3 are maximum and that of 2,6-DNT minimum. The detection limit for all these four explosives

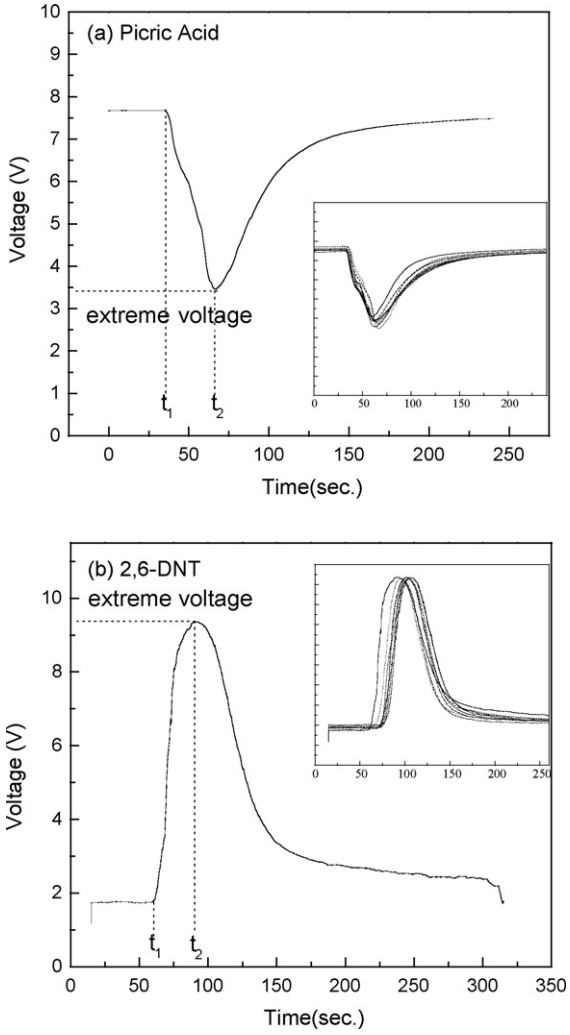

Fig. 2. Typical dynamic response curves for the explosives: (a) picric acid, and (b) 2,6-DNT. The inset shows the repeated eight response curves.

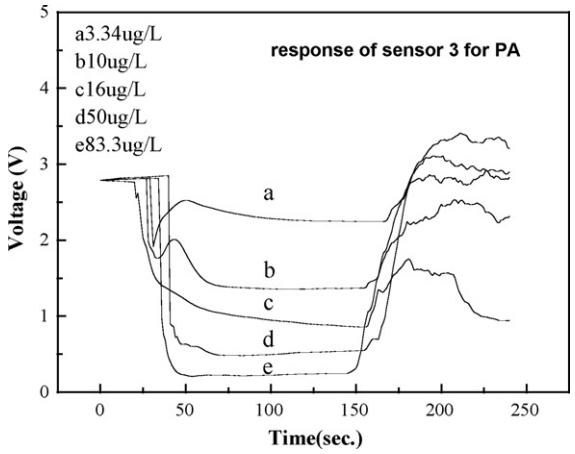

Fig. 3. The typical static-state response curves for sensor 3 at different concentrations of picric acid.

are low to 3.34 μg/L, and the sensitivity is the exponential function of the decomposed gas concentration. The results imply that there are potential applications for ZnO-based nanoparticle sensors as highly sensitive elements for the alarm of explosives at very low concentrations. Among these six sensors, the sensor 4 (WO_3-doped ZnO sensor) almost showed the highest sensitivity for the three oxidizing signal explosives, whose sensitivities were 14 (Fig. 4(c)), 8.5 (Fig. 4(b)), and 7 (Fig. 4(a)) for NH_4NO_3, ME, and PA at the concentration of 83.34 μg/L, respectively. However, for the reducing signal explosive (2,6-DNT) (Fig. 4(d)), the sensor 2 and sensor 3 showed better sensitivity, whose values were 2.5 and 3.0, respectively. Sensor 1 and sensor 6 showed plain sensitivity and selectivity for the tested four explosives. Just due to these differences from the six sensors sensitive to the four explosives, there is possibility to classify and discriminate the four explosives by using the appropriate pattern-recognition algorithm. The interaction mechanism between gas sensors and explosives could not be clearly explained by day of our manuscript submission.

The DFA method is a commonly used technique for data classification and dimensionality reduction. It was employed to classify and discriminate the four explosives at the concentrations of 83.3 and 3.34 μg/L after eight repeated tests at each concentration point. The sensitivity, *S*, is selected as an input parameter. The classified and discriminate results are shown in Fig. 5. It is apparent in Fig. 5(a) that data points segregated into four distinct, non-overlapping groups for the individual explosives. The results showed that the four tested explosives could be well classified and discriminated at the concentration of 83.3 μg/L. Under our investigation, the four explosives can be completely separated over 10 μg/L (figures not shown). But in Fig. 5(b) there seemingly are three unattached clusters: one for PA, one for ME, and the other for 2,6-DNT and NH_4NO_3 together. In fact, the point spaces for the four explosives are partly overlapped each other. For example, a few points for PA rambled into the cluster for 2,6-DNT and one point for NH_4NO_3 into the cluster for ME. It implied that these four explosives couldnot be identified at the concentration of 3.34 μg/L by using DFA method. The DFA result also reports that there is only 65.6% success rate in classification of each single explosive. The

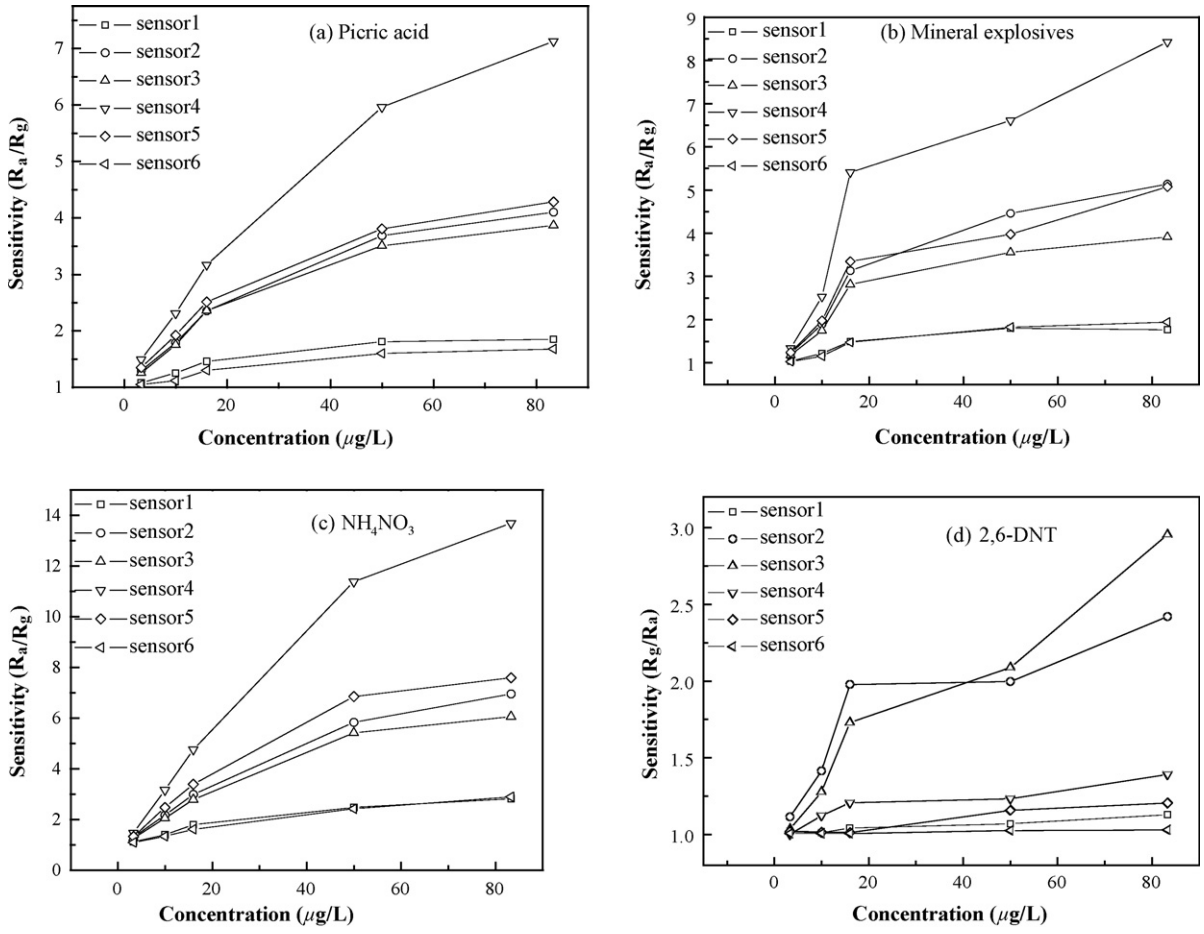

Fig. 4. The sensitivity of the six sensors to various concentrations of the four explosives (a) picric acid, (b) mineral explosives, (c) NH_4NO_3, and (d) 2,6-DNT.

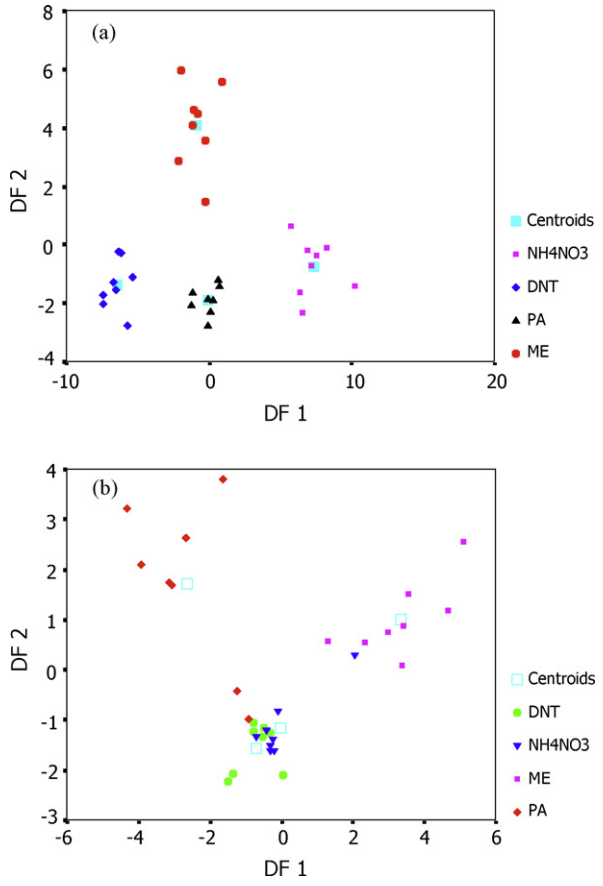

Fig. 5. DFA results of sensitivity at the concentrations of 83.3 and 3.34 μg/L for static sampling experiments: (a) at the concentrations of 83.3 μg/L, and (b) at the concentrations of 3.34 μg/L.

reason may be that the sensitivity is too low to show difference at low concentration. Further classification and discrimination of lower concentration should be appealed to new sensing materials and technology including pattern classification method.

3.3. Dynamic sampling experiments

The air flows of the two lines are tuned by the MFC2/MFC1 flow ratios of 600/30, 700/30, 800/30, 900/30, and 900/10. The concentrations of diluted explosives should be obtained as follows:

$$C_{\mathrm{lm}} = \frac{4.0\ \mathrm{mg}}{60\ \mathrm{ml}} \times 10\ \mathrm{s} \times \frac{B\ \mathrm{ml}}{60\ \mathrm{s}} \times \frac{B}{A+B} \times \frac{1}{700\ \mathrm{ml}} \times 10^6 \quad (3)$$

where 4.0 mg is the weight of raw explosive analyte; 60 ml the volume of the sampling bottle; 10 s the maximum time of the lingering decomposed gas over the gas sensors; B ml/60 s the flow ratio controlled by MFC1; $B/(A+B)$ the diluted ratio of the decomposed gas (A = 600, 700, 800, and 900; B = 30 and 10); 700ml the volume of the testing chamber. The last unit of this expression is μg/L. Thus, the concentrations, C_{lm}, corresponding to the flow ratios of 600/30, 700/30, 800/30, 900/30, and 900/10 should be 22.7, 19.6,17.2, 15.4, and 1.7 μg/L.

Due to the too low testing signals of the sensors at the concentration of 1.7 μg/L, the test was repeated eight times at the concentration of 15.4 μg/L. The response curves are similar with that in Section 2.2 (shown in Fig. 2) but smaller signals. From the dynamic curves, we proposed the slope between t_1 and t_2 as the feature parameter and extracted the maximum value of slopes for each curve as an input vector to classify the four explosives. The classified and discriminated results at the concentration of 15.4 μg/L are shown in Fig. 6. It is reported that the four explosives can be classified and discriminated for 100% success rate at this concentration. The results are consistent with that of the static-state experiments, whose detection levels are both in μg/L. This experiment approached much closer to the practical application and the future work would be devoted to the lower concentration detection of the explosive and the miniaturization of the testing setups.

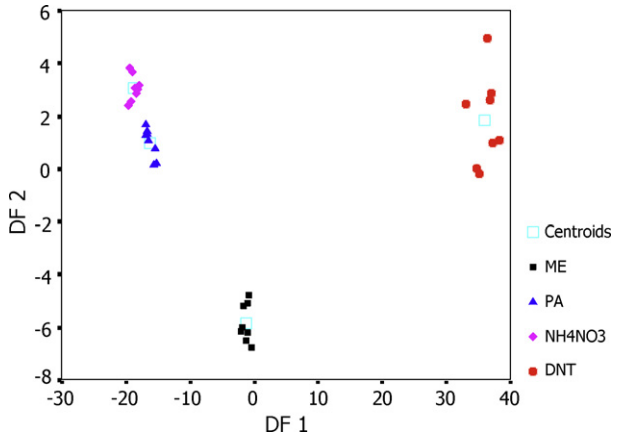

Fig. 6. DFA results of sensitivity at the concentrations of 15.4 μg/L for dynamic sampling experiments.

4. Conclusions

The ZnO-doped nanoparticle sensors with additives of Sb_2O_3, TiO_2, V_2O_5, and WO_3 were prepared to test the four representative explosives (NH_4NO_3, mineral explosives, picric acid and 2,6-DNT). An optimized sensors array was obtained after repeated test and selection. With static-state and dynamic sampling experiments and some repeated measurements, conclusions can be achieved as follows:

WO_3-doped ZnO nanoparticle sensor revealed the good sensitivity for the three oxidizing signal explosives, whose sensitivities were 14, 8.5, and 7 for NH_4NO_3, ME, and PA at the concentration of 83.34 μg/L, respectively. However, for the reducing explosive (2,6-DNT), the pure ZnO nanoparticle sensor (sensor 2) and ZnO-doped nanoparticle sensors with TiO_2 (sensor 3) showed better sensitivity, whose value was 2.5 and 3.0, respectively. ZnO-doped nanoparticle sensors could detect the explosives with the low concentration of 3.34 μg/L. With the help of DFA method, the four explosives could be well classified and discriminated at the concentration of 83.34 μg/L. To approach closer practical application, full dynamic sampling experiments were carried out and the results demonstrated that all samples could be identified completely at 15.4 μg/L when extracting maximum of slope as the feature to DFA.

New gas-sensing material and technique will be focused on to detect lower concentration explosives and to make the device portable in the future work.

Acknowledgements

The authors gratefully acknowledge the financial support by Nature Science Foundation of China (Nos. 50041024 and 50271029).

References

[1] J.N. Goodrich, Attack on America: a record of the immediate impact and reactions in the USA travel and tourism industry, Tourism Manage. 23 (2002) 573–580.

[2] G.A. Eiceman, J.A. Stone, Ion mobility spectrometers in national defence, Anal. Chem. A 76 (2004) 390–397.
[3] J. Yinon, Detection of explosives by electronic noses, Anal. Chem. A 75 (2003) 98A–105A.
[4] S. Content, W.C. Trogler, M.J. Sailor, Detection of Nitrobenzene, DNT, and TNT vapors by quenching of porous silicon photoluminescence, Chem. Eur. J. 6 (2000) 2205–2213.
[5] M. Nipper, Y. Qian, R. Scott Carr, K. Miller, Degradation of picric acid and 2,6-DNT in marine sediments and waters: the role of microbial activity and ultra-violet exposure, Chemosphere 56 (2004) 519–530.
[6] M.R. Darrach, A. Chutjian, G.A. Plett, Trace explosives signatures from world war II unexploded undersea ordnance, Environ. Sci. Technol. 32 (1998) 1354–1358.
[7] Suman Singh, Sensors—an effective approach for the detection of explosives, J. Hazard. Mater. 144 (2007) 15–28.
[8] B.L. Zhu, C.S. Xie, W.Y. Wang, K.J. Huang, J.H. Hu, Improvement in gas sensitivity of ZnO thick film to volatile organic compounds (VOCs) by adding TiO_2, Mater. Lett. 58 (2004) 624–629.
[9] M. Garcia, M. Aleixandre, J. Gutieĭrrez, M.C. Horrillo, Electronic nose for wine discrimination, Sens. Actuators B 113 (2006) 911–916.
[10] Q.Y. Zhang, C.S. Xie, S.P. Zhang, A.H. Wang, B.L. Zhu, L. Wang, Z.B. Yang, Identification and pattern recognition analysis of Chinese liquors by doped nano ZnO gas sensor array, Sens. Actuators B 110 (2005) 370–376.
[11] http://demining.jrc.it/aris/events/mine99/program/P82-86/p82-86.htm.
[12] L Senesac, T.G. Thundat, Nanosensors for trace explosive detection, Mater. Today 11 (2008) 28–36.
[13] M. Krausa, K. Schorb, Trace detection of 2,4,6-trinitrotoluene in the gaseous phase by cyclic voltammetry, J. Electroanal. Chem. 461 (1999) 10–13.
[14] J.R. Stetter, S. Strathmann, C. McEntegart, M. Decastro, W.R. Penrose, New sensor arrays and sampling systems for a modular electronic nose, Sens. Actuators B 69 (2000) 410–419.
[15] Y.H. Gui, C.S. Xie, A novel simplified method for preparing ZnO nanoneedles via H_2O_2 pre-oxidation, Mater. Chem. Phys. 93 (2005) 539–543.
[16] T. Gao, T.H. Wang, Synthesis and properties of multipod-shaped ZnO nanorods for gas-sensor applications, Appl. Phys. A 80 (2004) 1451–1454.